Original article

Folia Neuropathologica

The cycloid and skeletonization methods for morphometric analysis of fetal brain vessels

Tomasz Stępień[1], Boguslaw Obara[2,3]

[1]Department of Neuropathology, Institute of Psychiatry and Neurology, Warsaw, Poland; [2]Strata Mechanics Research Institute, Polish Academy of Sciences, Krakow, Poland; [3]Center for BioImage Informatics, Department of Electrical and Computer Engineering, University of California, Santa Barbara, USA

Folia Neuropathol 2008; 46 (4): 278-285

Abstract

In our study, we examined 54 images from 9 fetal brains from the 11th to 22nd gestation week (GW). We measured the length density (LD) of vessels (µm/µm2) in the cortical grey matter (CGM) and in the cortical white matter (CWM). The aim of this work was to find a method which could be applied to measure the length density of vessels on two-dimensional (2D) sections. The first method (cycloid method) was based on cycloid function based on Stereo Investigator Software (MicroBrightField). The length in 2D could be estimated on the basis of a number of intersections between a line-probe and the linear objects of interest. In the study, we used a line-probe with systematically spaced sine-weighted curves (cycloids) of known length. In this case, the cycloids were 53.1 µm long. The counting grid was constructed from sine-weighted lines (cycloids), which were used for estimation of the length density of vessels. The second method (skeletonization) was based on the mathematical functions of morphology and colour system transformation. The "binary airway tree" formed by the image segmentation step was skeletonized to identify two- or three-dimensional centrelines of individual branches, and to determine the branch point locations. The idea was to utilize a skeletonization algorithm which was based on properties of the average outward flux of the gradient vector field of a Euclidean distance function from the boundary of the structure. Both of these methods (cycloid and skeletonization) could be applied in measuring the length density of vessels on two-dimensional (2D) sections. These morphometric methods allowed us to measure the length density in fetal development of vessels in the cortical grey matter and the cortical white matter. The cycloid method could be applied to measure an approximate length density of vessels. However, skeletonization should be applied to measure more precisely length density of vessels in the cortical grey matter and the cortical white matter.

Key words: *image analysis, skeletonization, cycloid method, human fetal brain, vascular length density, CD34.*

Introduction

What is the objective of generating hundreds of digits resulting from microscopic image analysis? It turned out that the mere terms "large, medium, short" are insufficient in scientific discourse, which calls for unification of parameter description. Therefore, geometric features began to be used to describe the surface of objects in mathematical terms. This brought modern morphometry to life. Howe-

Communicating author:

Tomasz Stępień, Department of Neuropathology, Institute of Psychiatry and Neurology, Sobieskiego 9, 02-957 Warsaw, Poland, tel. +48 22 458 27 86, Email: tstepien@ipin.edu.pl, obara@ece.ucsb.edu

ver, it still did not answer the question of relations between objects in space. What was needed was a method of transposing geometric parameters from surface to space. This issue was first addressed by Count Buffon in the late 18th century. He made an experiment on needles scattered on the floor, suggesting that the number of intersections would be directly proportional to the length of the needle, and inversely proportional to the distance between the lines on the floor [5]. Buffon's problem provided the basis for length estimation in modern morphometry, allowing for quantitative description of a set of solids with measurements (e.g. of size or length) or counting based on 2D cross-sections of the solids.

In our study, we examined the length density of vessels in the fetal brain cortical grey matter (CGM) and the cortical white matter (CWM) in fetal brains between GW 11 and GW 22, using two methods. The first one was skeletonization, consisting in measuring objects on the surface, and the second one was the cycloid method, based on Buffon's experiment. The objects of our interest were blood vessels and their development. Normal vascular development in the brain plays an important role in the appropriate proliferation, migration and maturation of neurons, glial cells, in synaptogenesis and in building connections of various structures [9,11,19]. The development of the primitive vascular network in the brain involves two different mechanisms: vasculogenesis and angiogenesis. Vasculogenesis forms blood vessels from differentiating endothelial cells (ECs) from mesenchymal precursors (angioblasts/haemangioblasts). Angiogenesis is a process where vessels sprout and branch from pre-existing ECs and vessels [3,21,24,25]. Pathological vasculogenesis and/or angiogenesis during early prenatal development underlie the pathophysiology of many neurodevelopmental disorders [14,15,18]. The alteration of capillary length density in the fetal brain may tell us more about factors activated during development. In our study, we tried to establish which method proves useful to measure the length density of vessels on two-dimensional (2D) sections.

Material and Methods

Brain specimens

The cortical grey matter (CGM) and the cortical white matter (CWM) of frontal lobe from a group of 9 fetuses without neuropathological abnormalities were studied. Fetal brains ranging from gestation week (GW) 11 to 22 were fixed in 4% paraformaldehyde in 0.1 M phosphate buffer saline (PBS), pH 7.4. The fixed samples were then embedded in paraffin, and cut serially at 8 µm in frontal sections, which was followed by routine staining of brain tissue slices with haematoxylin-eosin (H&E) and immunohistochemical reaction with antibody CD34 (Novocastra 1:25). The gestational age in each case was calculated from the date of the last menstrual period.

Image analysis

Image analysis and processing techniques are successfully used in medical image analysis [6,7]. One of the most important parts of image analysis is skeletonization. The binary airway tree formed by the image segmentation step is skeletonized to identify the two- or three-dimensional centrelines of individual branches and to determine the branch point locations.

Skeletonization of three-dimensional tubular structures is reported by Palágyi et al. [17]. Palágyi's method specifically targets skeletonization of vascular- and airway tree structures in medical images. Bouix et al. [4] presented a fast, robust and automatic method for computing centreline paths through tubular structures, to be applied in virtual endoscopy. Bouix's idea is to utilize a skeletonization algorithm based on the properties of the average outward flux of the gradient vector field of a Euclidean distance function from the boundary of the structure. Soltanian-Zadeh et al. [20] proposed an image processing approach for information extraction from images of the vascular structure. Soltanian-Zadeh's method allows extraction of information such as skeleton length and diameter from real confocal microscopic images of the vessels in rat brains. Quantitative information revealed in angiograms, for example vessel length, diameter, course, and curvature, is essential and can be accessible by computer with image analysis methods, particularly skeletonization [16].

The thinning process is based on the Hit or Miss transform, which is a combination of erosion and dilation operators that allows a foreground pixel to be matched according to a predefined structuring element. Removing branches of the skeleton tree can be computed by iteratively detecting and removing the end points of the tree, until there are only two of them left. This method successfully removes short spurs from the skeleton but it can also discard end po-

ints of the skeleton main path, especially when branches are long. The main path is required to maintain its full length, i.e. to connect two pixel positions on the boundary of the original shape. To compute it, an algorithm based on the Euclidean distance between the end points of the skeleton and its nodes is used (Fig. 10). For each node (white colour), the distance between the node and each end point (black colour) is calculated. The end point with the minimum distance is then removed. With this technique, only the longest of all the branches starting from a given node are kept. This process is done iteratively until there is no more node, i.e. only two end points are left. The result of the whole process (Fig. 10D).

The dilation of a set *I* by a structuring element *B* is denoted as $\delta_B(I)$ and is defined as a locus of points *z* such that *B* hits *I* when its origin coincides with *z*.

$$\delta_B(I)=\{z : B_z \cap I \neq \varnothing\} \quad (1)$$

Erosion is defined as:

$$\varepsilon_B(I)=\{z : B_z \subset I\} \quad (2)$$

Based on erosion and dilation, we define opening and closing, which form the basis of morphological filtering. The opening of an image *I* by a structuring element *B* is defined as erosion of *I* followed by dilation with *B*.

$$\gamma_B(I)=\delta_B(I)\ \varepsilon_{B^T}(I) \quad (3)$$

Closing is defined as:

$$\varphi_B(I)=\varepsilon_B(I)\ \delta_{B^T}(I) \quad (4)$$

Opening by reconstruction is defined as:

$$\gamma_B^{rec}(I)=\rho_{(I,G)}\ \varepsilon_B(I) \quad (5)$$

where: $G=\varepsilon_B(I)$.

I image is reconstructed by the marker function *G*, by an infinite number of recursive iterations (iterations until stability) of the dilation of *G* conditioned by *I*.

Closing by reconstruction is defined as:

$$\varphi_B^{rec}=(\gamma_B^{rec}(I^C))^C \quad (6)$$

where: I^C – complement of *I*.

Top-hat is defined as:

$$T(I)=I-\gamma(I) \quad (7)$$

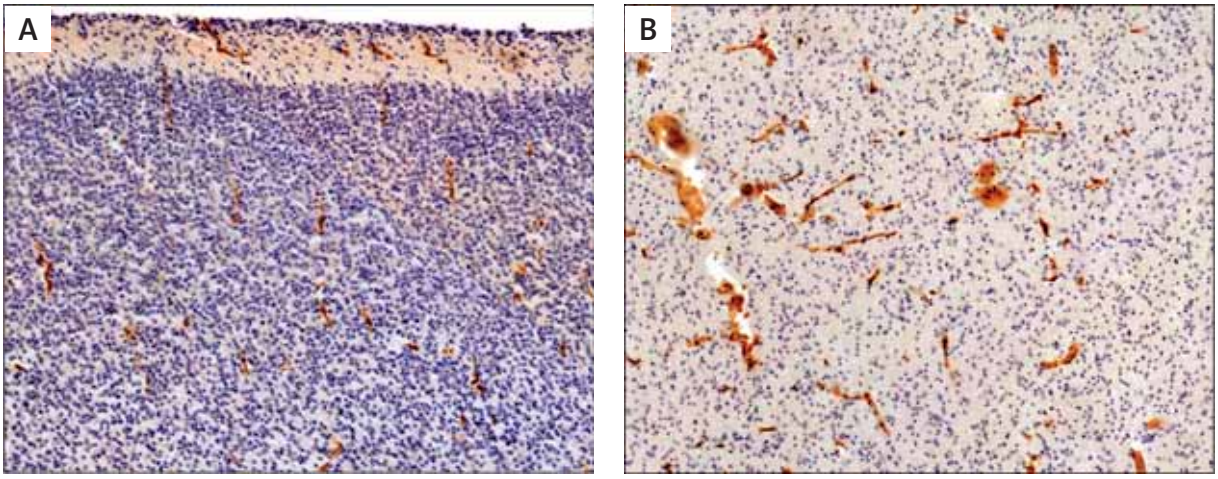

Fig. 1. Surface density of vessels. A. Cortical grey matter, B. cortical white matter. Immunohistochemical reaction with antibody CD34, ×200

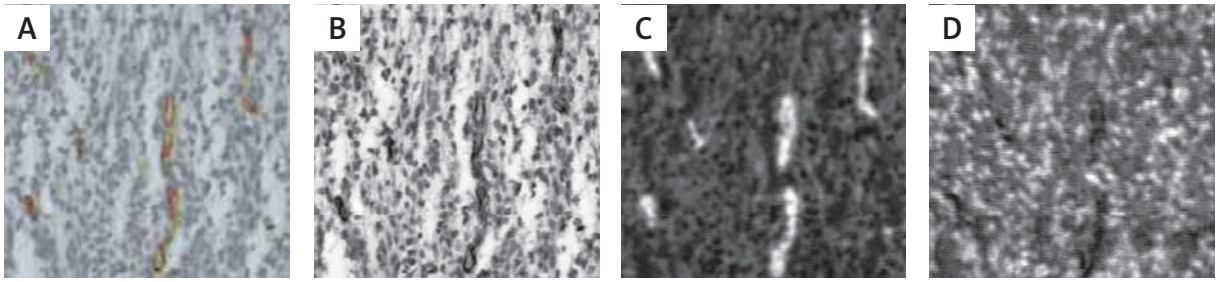

Fig. 2. Representation of input colour image (A) in YIQ colour space, B) Y, C) I, and D) Q components

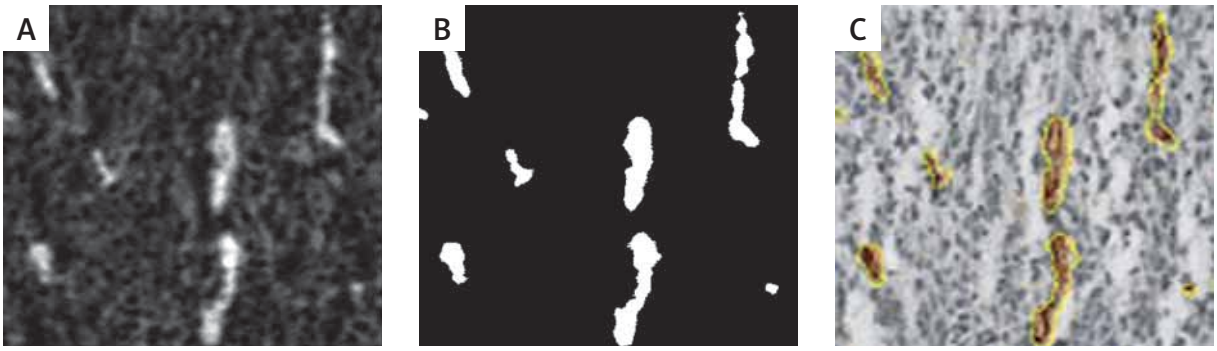

Fig. 3. Segmentation of I image (Fig. 2): A) top-hat, B) thresholding and C) result

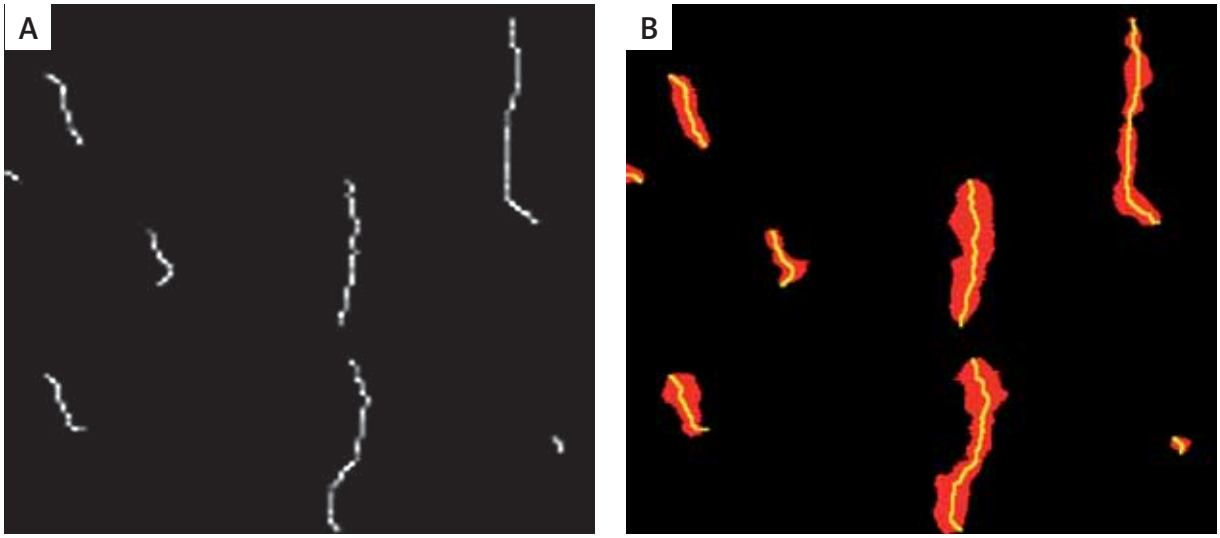

Fig. 4. Results of length estimation of figure 2A image: A) skeleton and B) overlay on figure 3C

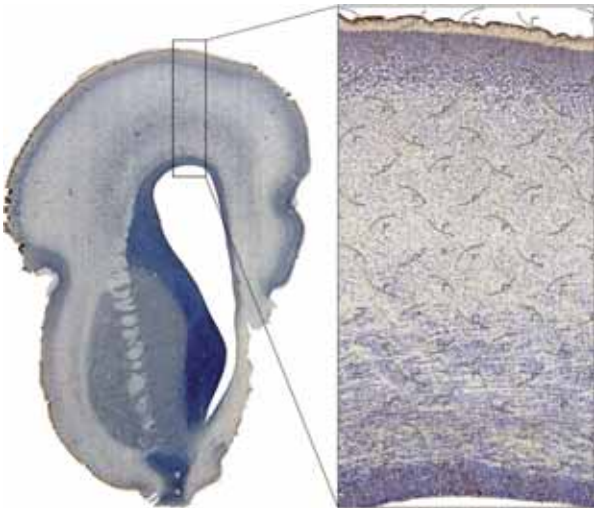

Fig. 5. A. Section with immunohistochemical reaction with antibody CD34 with haematoxylin contrast stain, B. surface with cycloid grid (×200)

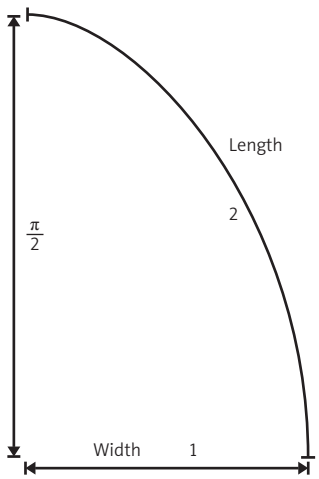

Fig. 6. Sine-weighted curves, cycloids

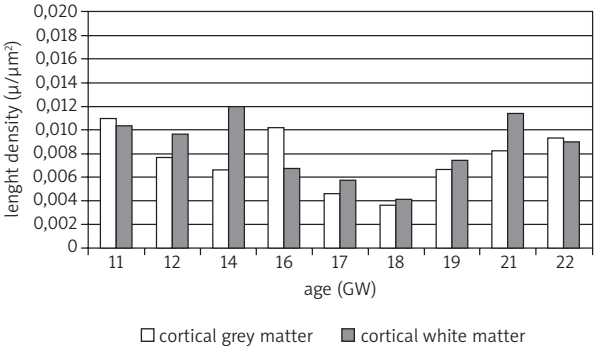

Fig. 7. Length density of vessels by cycloid method

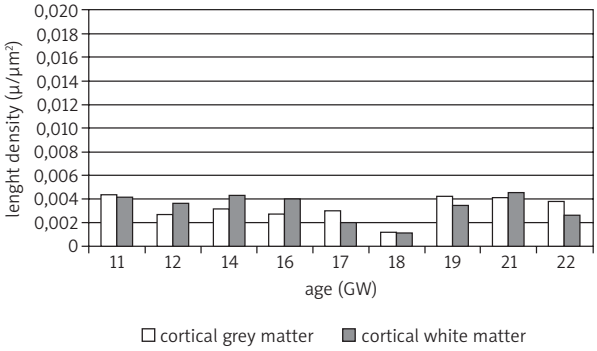

Fig. 8. Length density of vessels by skeletonization method

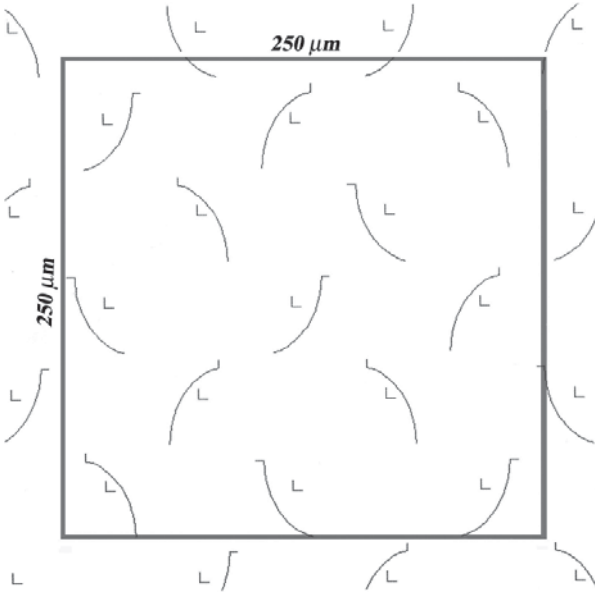

Fig. 9. Test square

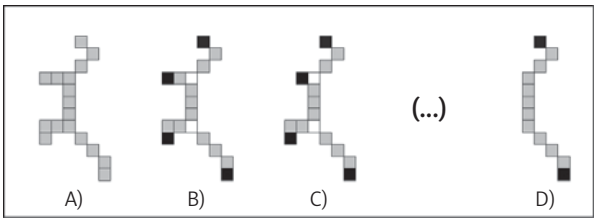

Fig. 10. Pruning method iterations: A) input skeleton, B) detected end points and nodes, C) first step of pruning, D) final step of pruning

In the paper, the author recapitulates the results of research of development and application of an image analysis tool for automatic segmentation and length estimation of 54 microscopic images of fetal brain vessels.

The image analysis and processing algorithms were applied to estimate the length of vessels of 54 microscopic images of fetal brain vessels. A sample of input image was used to present the main idea of the procedure. The RGB to YIQ colour system transformation was used as a pre-processing procedure for analysed images, where the YIQ representation of the image from Figure 2A is presented on Figures 2B, 2C and 2D.

The main steps of image segmentation procedure are shown in Figure 3. The image segmentation procedure was based on mathematical morphology. At first, the analyzed image was filtered by a morphological top-hat filter (Fig. 3A), then the image was thresholded and the result is shown in Figure 3B, 3C.

Segmented images of fetal brain vessels were used in the length estimation. The length analysis algorithm was based on a technique proposed by Fuller et al. [10]. They presented the techniques developed for automatic detection of filaments on Meudon Hα spectroheliograms, and, by extension, on any full-disk Hα Sun observations. The filaments were then segmented with a region growing method, which efficiently reflects the full extent of these dark areas. The filaments were finally described by means of their pruned skeleton. The length estimation of fetal brain vessels from Figure 2A, based on Fuller's method (Fig. 4).

Colour system transformation (C++ – author's implementation) and image analysis algorithms (Aphelion TM – C++ library) [1] were developed in Aphelion ADCIS software and used for the segmentation of the microscopic images of fetal brain vessels.

Cycloid method

Morphometry is a body of mathematical methods relating "geometrical parameters" (such as volume and surface area) of spatial objects to lower dimensional measurements obtainable on a section of the structure [2,23].

Morphometric methods enable one to estimate some parameters of anisotropic objects on a section. The length in 2D could be estimated on the basis of various intersections between a line-probe and the linear objects of interest [5].

In our study, we used the stereological method with systematically spaced sine-weighted curves (cycloids) of known length, in our case being 53.1 µm. The counting grid constructed of sine-weighted lines (cycloids) can be used with the vertical section for estimation of lengths and surface areas (Fig. 6). The cycloid test system lines on vertical sections have an *isotropic* orientation distribution within the *three-dimensional structure* [2]. The curve has parametric coordinates (θ – sin θ, 1 – cos θ) where θ is the angle between a test line segment and vertical axis.

All sections were collected using a 20x- magnifying objective. The surface density of vessels (Fig. 5B) is estimated on the basis of intersections between the cycloids and the brain surface and the number of test points (crosses at each end of cycloid arcs). To avoid bias, all cycloids must be positioned equally randomly with respect to the section and their minor principal axis must be parallel to the selected vertical axis [22]. The final calculation of length density of vessels was a result of multiplying two times the sum of total intercepts and area per unit cycloid length through the section sampling fraction and the area sampling fraction.

$$L_V = 2\frac{[\bar{I}_L^C]_{\rho\eta}}{\Delta} \tag{1}$$

$$L_V = \frac{2}{\Delta}\bullet\frac{(\bar{I}^{C\chi}{}_C)_{\rho\eta}}{\bar{P}\bullet(l/p)} = \frac{2}{\Delta}(p/l)\frac{\sum_{i=1}^{n} I_i}{\sum_{i=1}^{n} P_i} \tag{2}$$

$$\widehat{V} = m\Delta(\frac{a}{p})\sum_{i=1}^{n} P_i \quad \widehat{L} = 2(\frac{a}{l})m\sum_{i=1}^{n} I_i \tag{3}$$

$$CE(L_V) = \sqrt{\frac{n}{n-1}\left(\frac{\sum_{i=1}^{n} I_i^2}{\sum_{i=1}^{n} I_i \sum_{i=1}^{n} I_i} + \frac{\sum_{i=1}^{n} P_i^2}{\sum_{i=1}^{n} P_i \sum_{i=1}^{n} P_i} - 2\frac{n\sum_{i=1}^{n} I_i P_i}{\sum_{i=1}^{n} I_i \sum_{i=1}^{n} P_i}\right)} \tag{4}$$

p/l – test points per unit length of cycloid, n – number of probes, I_i – intercepts, P_i – test $[\bar{I}_L^C]\rho\eta$ – mean intercepts of projected images per unit length of cycloid, Δ – section thickness, points.

$$estL_{cap} = 2\frac{a}{l}\sum l\bullet\frac{1}{ssf}\bullet\frac{1}{asf}\bullet\frac{t}{h} \tag{5}$$

$$asf = \frac{area\left(Frame\right)}{area\left(x, y\,step\right)} = \frac{x_{CF}\bullet y_{CF}}{x_{step}\bullet y_{step}} \tag{6}$$

where *estL* = total length of capillaries (µm), $\frac{a}{l}$ – area per unit cycloid length, Σl – total intercepts, *ssf* – section sampling fraction, *asf* – area sampling fraction, *t* – section thickness, *h* – height of counting frame

Photography

Photos shown in Figure 1 were produced by a digital photography workstation. Photomicrographs (Fig. 5A-B) were produced by digital photography using an Olympus U-CMAD-2 digital camera attached to an Olympus AX 70 microscope. The final figures were constructed using Photoshop v.7. Adjustments of contrast and brightness were made to facilitate recognition of the immunohistochemical signal at low high magnification, without altering the appearance of the original materials. The images were registered in RGB (red, green, blue) colour system with standard resolution of 10 000×10 000 pixels.

Results

We analyzed 54 images of 9 fetal brains aged 11 to 22 GW. The morphometric measurements were performed on 2D pictures of samples marked with CD34. In our research, we used two morphometric image analysis methods. Only CD34 marked blood vessels were included in counting. In the cases studied with the cycloid method, there were major fluctuations observed between 11 GW (CGM – 0.01095 µ/µm^2; CWM – 0.01034 µ/µm^2) and 22 GW (CGM – 0.009361 µ/µm^2; CWM – 0.00900 µ/µm^2) (Fig. 7). A remarkable drop in length of blood vessel network density was observed in GW 17 and 18. Changes in the length of blood vessel network density in GW 11 to 16 (CGM – 0.01020 µ/µm^2;

CWM – 0.00672 μ/μm²), both in the cortical grey matter and in the cortical white matter, did not prove statistically significant. However, the reduction of the length of blood vessel network density in GW 17 (CGM – 0.00466 μ/μm²; CWM – 0.00577 μ/μm²) and in GW 18 (CGM – 0.00367 μ/μm²; CWM – 0.00407 μ/μm²), both in the cortical grey matter and in the cortical white matter, proved significant. We found statistically significant changes between GW 11 and GW 17 (CGM – $p<0.039$; CWM – $p<0.01$), as well as between GW 11 and 18, in the length of blood vessel network density (CGM – $p<0.0087$; CWM – $p<0.001$). We also established statistically significant differences in the length of blood vessel network density between GW 17 and 21, both in the cortical grey matter and in the cortical white matter (CGM – $p<0.01$; CWM – $p<0.002$), as well as between GW 17 and 22 (CGM – $p<0.019$; CWM – $p<0.03$). We got similar results when comparing the length of vascular network density between GW 18 and 21 (CGM – $p<0.004$; CWM – $p<0.001$). Also, between GW 18 and 22, the difference in the length of vascular network density showed statistical significance (CGM – $p<0.004$; CWM – $p<0.003$), whereas it did not between GW 14 (CGM – 0.00660 μ/μm²) and GW 18 (CGM – 0.00367 μ/μm²) as regards the cortical grey matter. Next, we analyzed the test sample using skeletonization (Fig. 8). The results did not show as high fluctuations as in the cycloid method analysis. The length of vascular network density between GW 11 (CGM – 0.00434 μ/μm²; CWM – 0.00419 μ/μm²) and GW 16 (CGM – 0.00273 μ/μm²; CWM – 0.00405 μ/μm²), both in the cortical grey matter and in the cortical white matter, is similar. What is remarkable, however, is the drop in length density of the vascular network in GW 18 (0.001189 μ/μm²), both in the cortical grey matter and in the cortical white matter. The increase in the vascular network length density in the cortical grey matter is similar between GW 19 (CGM – 0.00426 μ/μm²) and GW 22 (CGM – 0.00385 μ/μm²), whereas in the cortical white matter it is sinusoidal, reaching an extreme in GW 21 (0.00452 μ/μm²) and dropping in GW 22 (CWM – 0.00266 μ/μm²).

Discussion

Skeletonization and cycloid methods could be successfully applied in 2D image analysis. In our study in the cortical grey matter with the cycloid method were on average 45% higher than those from skeletonization and as much as 57% higher in the cortical white matter (Table I). Such different results made us use both methods in analyzing objects of known length. Thus, we measured the circumference of a square of 250 μm side by skeletonization (1000 μm) and by cycloid method (1319 μ m) (Fig. 9). The outcome confirmed the differences in the study results, which stem from the algorithms used. Skeletonization, consisting in selecting axial points (skeletons) of figures, allows for measurement of absolute length of objects on the surface (Fig. 10) [16], whereas the cycloid method, included in Stereo Investigator Software (MicroBrightField), is a method of estimation which consists of a known-length cycloid grid and counting intersection points (Fig. 5B). This procedure has a high error burden and should be used only very cautiously in 2D

Table I. Comparison lenght density of vessels network by cycloid and skeletonization method

Age (GW)	Lenght density of vessels (μ/μm²)			
	cycloid method		skeletonization method	
	cortical gray matter	cortical white matter	cortical gray matter	cortical white matter
11	0.01095	0.01034	0.00434	0.00419
12	0.00766	0.00968	0.00275	0.00365
14	0.00660	0.01192	0.00318	0.00432
16	0.01020	0.00672	0.00273	0.00405
17	0.00466	0.00577	0.00301	0.01139
18	0.00367	0.00407	0.00119	0.00115
19	0.00664	0.00743	0.00426	0.00352
21	0.008198	0.01139	0.00410	0.00452
22	0.009361	0.00900	0.00385	0.00266

image morphometric analysis. A good solution seems to be skeletonization, which enables absolute length densities of studied blood vessels to be specified in 2D images. In both methods, we observed a remarkable drop in length density of vascular network in GW 18. This may be explained by intensive migration of neurons and glial cells and delayed angiogenesis, which changes the relation between blood vessels and the surface of the section, and which might result in reduced vascular length density. The reduction of vascular length density might result from developmental atrophy of blood vessels, combined with their differentiation [8]. In such a case, the vascular atrophy might consist of vascular endothelial cells (VECs) in apoptosis [13], which results from reduced vascular flow and macrophage function [12]. Morphometric studies may be a good tool for analyzing vasculogenesis and angiogenesis in the brain development process. The cycloid method could be applied to measure approximate length density of vessels. However, skeletonization should preferably be applied to measure the precise length density of vessels in the cortical grey matter and the cortical white matter.

Acknowledgement

The manuscript was greatly improved by comments and suggestions made by Prof. R. Tadeusiewicz. The study is supported by the Polish State Committee for Scientific Research through the statutory research foundation.

References

1. Aphelion TM., 2005. http://www.adcis.net/Products/Aphelion/GeneralDescription.html
2. Baddeley AJ, Gundersen HJG, Cruz-Orive LM. Estimation of surface area from vertical sections. J Microsc 1986; 142: 259-276.
3. Baldwin HS. Early embryonic vascular development. Cardiovas Res 1996; 31: E34-E45.
4. Bouix S, Siddiqi K, Tannenbaum A. Flux driven automatic centerline extraction. Med Image Anal 2005Ł 9: 209-221.
5. Buffon GL. Essai d'Arithmetique Morale (Supp. Historie Naturelle vol. 4). Imprimerie Royale, Paris 1777.
6. Costaridou L. Medical Image Analysis Methods. Crc Press Llc 2005.
7. Dhawan A. Med. Image Anal. Wiley-IEEE Press 2000.
8. Feinberg R, Nolden D. Experimental analysis of blood vessel development on avian wing bud. Anat Rec 1991; 231: 136-144.
9. Friedl P. Prespecification and plasticity: shifting mechanisms of cell migration. Curr Opin Cell Biol 2004; 16: 14-23.
10. Fuller N, Aboudarham J, Bentley RD. Filament recognition and image cleaning on meudon h alpha spectroheliograms. Solar Physics 2005; 227: 61-73.
11. Ikeda E, Flamme I, Risau W. Developing brain cells produce factors capable of inducing the HT7 antigen, a blood-brain barrier-specific molecule, in chick endothelial cells. Neurosci Lett 1996; 209: 149-152.
12. Lang RA, Bishop MJ. Macrophages are required for cell death and tissue remodeling in the developing mouse eye. Cell 1993; 74: 453-462.
13. Lang RA, Lustig M, Francois F, Sellinger M, Pleksen H. Apoptosis during macrophage-dependent tissue remodeling. Dev 1994; 120: 3395-3403.
14. Miyawaki TM, Takashima S. Developmental characteristics of vessels density in the human fetal and infant brains. Early Hum Dev 1998; 53: 65-72.
15. Niemi LT, Suvisaari JM, Tuulio-Henriksson A, Lőnnqvist JK. Childhood developmental abnormalities in schizophrenia: evidence from high-risk studies. Schizophr Res 2003; 60: 239-258.
16. Obara B, Nizankowski RT. Application of image analysis methods to vascular blood flow analysis in angiographic imaging. Image Processing in Industrial Information Technology, Warsaw, Poland. Warsaw 2004, pp. 76-78.
17. Palágyi K, Tschirren J, Hoffman EA, Sonka M. Quantitative analysis of pulmonary airway tree structures. Comput Biol Med 2006; 36: 974-996.
18. Rapoport JL, Addington AM, Frangou S, Psych MR. The neurodevelopmental model of schizophrenia: update 2005. Mol Psychiatry 2005; 1-16.
19. Rosenstein JM, Krun JM. New roles for VEGF in nervous tissue – beyond blood vessels. Exp Neurol 2004; 187: 246-253.
20. Soltanian-Zadeh H, Shahrokni A, Khalighi M, Zhang ZG, Zoroo RA, Maddah M, Chopp M. 3-D quantification and visualization of vascular structures from confocal microscopic images using skeletonization and voxel-coding, Comput Biol Med 2005; 35: 791-813.
21. Urbich C, Dimmeler S, Endothelial Progenitor Cells functional characterization. Trends Cardiovasc Med 2004; 14: 318-322.
22. Vesterby A, Kragstrup J, Gundersen HJG, Melsen F. Unbiased stereologic estimation of surface density in bone using vertical sections. Bone 1987; 8: 13-17.
23. Weibel E. Stereological Methods. Vol.1: Practical Methods for Bilogical Morphometry. Academic Press, London 1979.
24. Wierzba-Bobrowicz T, Lewandowska E. Morphological study of endothelial cells in human the human fetus during early period of gestation. Folia Neuropathol 1995; 33: 241-245.
25. Zygmunt M, Herr F, Münstedt K, Liang U, Liang OD. Angiogenesis and vasculogenesis in pregnancy. Eur J Obst Gyecol Repr Biol 2003; 110: S10-S18.